International Research Journal of Engineering and Technology (IRJET) e-ISSN: 2395-0056
Volume: 13 Issue: 08 | Aug 2026 www.irjet.net p-ISSN: 2395-0072

Optimal cyclic reflux operational policy for ternary mixtures separation. 2. Minimum azeotrope mixture

Marija Stojkovic[1]

[1]*10, Impasse de Copenhague, 53100 Mayenne, France*

Abstract - *The optimal control strategy for the separation of a 1.0-1a class mixture in different configurations, namely regular batch rectifier and mixed configuration composed of a high-pressurized inverted column connected to the batch rectifier, has been presented. The above-mentioned configurations give similar recovery rates for both acetone/methanol production; however, to obtain highly purified products, the mixed configuration should be chosen. At first, the influence of the reboiler volume on the single-column configuration brought: with the doubling of reboiler volume, there is a significant increase in recovery rate by 33.32%, and interestingly, the overall time horizon reduction is almost the same. Furthermore, the influence of vapor boil-up showed that with the increase of vapor boil-up by 3.34 times, there is a significant increase in recovery rate by 20.90%, whilst a significant reduction of overall time horizon by 20.66% for total recovery. The influence of the pressure gap on elevated pressures on the double column configuration: with a pressure decrease of 10%/20%, resp., there is a significant increase in recovery rate by 12.09%/18.22%, resp., and it also gives 21.53%/31.33%, resp., in time reduction. Finally, the pressure gap on vacuum pressures set up an influence on the yield: with a pressure decrease of 10%/50%, resp., the total time for a maximum recovery is reduced by even 22.55%/2.259 times, resp.*

Key Words: multicomponent distillation, optimal control, methanol, 1.0-1a class, azeotrope

1. INTRODUCTION

In order to preserve the standard of living of mankind, it is necessary to produce large amounts of energy. Oil, natural gas, and coal still represent the main sources of energy and raw material for many derivatives' production. However, these raw materials are represented in limited quantities and are not renewable. The results are the instability of the global market and the increase in the price of fuel. Furthermore, significant amounts of greenhouse gases are produced by burning fossil fuels. For these reasons, all possible alternatives must be explored in order to find cost-effective and long-term solutions. Alternative fuels can be a solution for all major energy needs and for the demands of the growing world population as well as a way to reduce environmental pollution. Methanol belongs to one of the most common liquid fuels; therefore, this paper will be dedicated to the separation and/or purification of methanol in different configurations by the pressure-swing process.

You et al. (2014), focused their research on continuous mode only, to discover: 1) In the first step, there are the improvements if instead of extractive column only, the regeneratie column is also included since it brings 4.27%/6.81%, resp., savings in entrainer feeding rate/reflux ratio for regeneration column, resp., and 2) For the third step, all key variables, ie. entrainer feeding rate, reflux ratio for the regeneration column and reflux ratio for extractive column are sensitive to the three feed stages location (entrainer feed, mixture feed, regenerative feed), for example locations 31/49/18, resp., brings the improvement in entrainer feeding rate/reflux ratio for extractive column/reflux ratio for regenerative column/objective function, resp., for 11%/13,48%/10.53%/8.7%, resp., compared to the location at 25/40/14. You et al. (2015), reworked the closed-loop case from You2, for the top pressure set up at vacuum pressure of 0.6 [atm] in open-loop simulation: the latter given the reduction in the optimal entrainer feeding rate and objective function, for 29.74%/7.51%, respectively.

Daosud et al. (2016), compared neural network-based model predictive control with neural network direct inverse model control and proportional integral derivative control, even though the objective is no beter than 2%. it is proven that the first one provides the best operation in terms of stability. Tututi-Avila et al. (2017), examined an extractive distillation system with thermal coupling based on a system with a side rectifier, and an alternative extractive distillation system that assumes thermal coupling between two conventional distillation units: energy reduction achieved is 31.3%/39%, for the first/second configuration, resp., which translated in total annual cost reduction by 29.2%/33%, respectively.

Mangili et al. (2018), worked on three different configurations, to compare one to another in terms of energy reduction, CO_2 emissions, and water consumption: a newly invented energetically integrated extractive distillation brought more in energy reduction by 16%/24%, resp.; in CO_2 consumption reduction by 14%/23%, resp.; and water consumption reduction by 12%/26%, resp.; compared to conventional extractive distillation and pressure-swing distillation, resp. Frolkova et al. (2021), named the case where entrainer mixed with the original mixture in a reboiler, as "autoextractive distillation", and provided a study for the influence of the entrainer to feed ratio on energy consumption: for an increase in entrainer to feed ratio of 73.65%, there is a decrease in energy demand by

53.76%. Zhao et al. (2021), examined the separation of two minimum-boiling azeotropes in a triple-column-integrated quasi-continuous scheme using classical control, i.e., three pressure controllers to maintain the top pressures of the respective columns by manipulating condenser duty and two composition controllers by trial-and-error method to maintain the purity of the desired products. The authors achieved a significant 17.37% CO_2 reduction, compared to the scheme that consisted of a multi-vessel column connected to the double rectifier, only after full heat integration. Schöneberger et al. (2022), attempted to describe the behavior of a real plant, starting from a short-cut model to building step by step a high-fidelity model implemented in commercial software.

Zhang et al. (2022), attempted to improve the pressure-swing process by thermal coupling: the full scheme achieved a 50% reduction in total time compared to the partial scheme, better coped with feed disturbances, and reduced the total annual cost by 39.97% compared to the scheme without thermal coupling. Miao et al. (2022), introduced a hybrid heat-integrated process with two vapor compressors and no reboiler, and invented a novel method, an improved genetic algorithm, that combined genetic algorithm with particle swarm optimization, pattern search, and differential evolution: it gave a reduction in total annual cost and thermodynamic efficiency, by 30.6%/13.3%, resp., compared to a full heat integrated scheme. Even more importantly, the applied novel method gave different improvements for different mixtures examined, minimum boiling and maximum boiling azeotrope, whereas there is a gap of almost 10% between the novel method and the genetic algorithm applied to the maximum boiling azeotrope, whereas the values rest close for the minimum boiling azeotrope. Similarly, Seihoub et al. (2024), examined the same mixtures as previous authors, in conventional extractive columns and extractive dividing columns: the total energy duty calculated is close for minimum boiling azotrope (less than 2%), but there is an improvement by 12.45% for maximum boiling azeotropes, which makes us convinced that the more the mixture deviation from ideality, the more significant the improvements.

Ai et al. (2023), succeeded in removing methanol from the minimum boiling azeotrope by performing a specific two-step transesterification reaction, which yielded the main product, phenylcarbonate, and two byproducts, phenol and dimethyl carbonate. Hegely et al. (2023), invented a surrogate model-based method: dynamic model is incorporated into commercial software of ChemCad, in a set of points generated by Latin hypercube sampling in the space of optimization variables, and, algebraic equations were fitted by Automatic learning of algebraic model machine technique to describe objective function and constraints, finally to solve the problem with sequential quadratic programming method. Hegely et al. (2023), tested the integration of a heat pump in pressurized columns: interestingly, the case with bypass and heat pump integrated solely in a high pressurized column brought close total annual cost as the case where heat pumps were integrated in both columns; moreover, the removal of bypass brought additionally 12.33% of reduction. Hegely et al. (2025), proved that a progressively reduced-pressure policy reduces steam/incineration costs by at least 43.75%/22.7%, resp., compared to operation at atmospheric/vacuum pressure, resp. Hegely and Lang (2025), reworked the case from Hegely et al. (2023), with the surrogate model, to obtain the optimal total annual cost for different desired purities of distilled azeotrope component: the authors discovered that it reaches a maximum/minimum, resp., for the highest/lowest, resp., allowed composition in charge, or the improvement by 20.7%. Karaman et al. (2025) exploited the possibility of the feed composition within the azrotropic being introduced into high- and low-pressure columns, resp., to prove that the latter, after partial heat integration, is better in terms of total annual cost/CO_2 emissions by 8.47%/4.02 %, resp.

Luyben (2025) discovered that vapor density plays an important role in the modeling of pressure-swing distillation columns: it appears to be smaller at lower vapor pressure, which increases vapor velocity and thus the required diameter. Or, for an increase in diameter by 18.15% only, the reflux ratio must decrease by 2.36 times, and total annual cost by 38.31%. Liang et al. (2024), focused only on heat-integrated vaccum pressure processes: enhanced partial heat integration brought improvements in cost saving, CO_2 emissions, and energy efficiency enhancement by 8.4%/6.6%/20.5%, resp., compared to enhanced full heat integration. Wen et al. (2025), prior to classical dynamic control performance analysis, evaluated the process set-up, i.e., three pressure-swing processes with different sequences by inventing a minimum distance method: acknowledged that relative locations between the feed compositions and distillation boundaries in each region are very different, normal distance is a parameter to be used in performance evaluation. For a specific process, methanol-ethylacetate-cyclohexane separation, with normal distance increase by only 15.05%, the total annual cost and reboiler duty are reduced by 23.8%/26.4%, resp.

Mahida et al. (2025), examined the casses of different initial charge composition, for the mixture where two components are from very close boiling temperature, whereas the first/second/third component resp., is in excess in the mixture: the authors concluded that total reboiler duty is higher for the process where water component is in excess, compared to the cases where formic acid/propionic acid are in excess by 2.0/2.1 times, resp., or the most optimal distribution of energy consumption among the columns is provided in the case of propionic acid rich mixture (lower boiler). Jassim et al. (2025), researched methyl salicylate production in batch and semi-batch configurations: only the latter mode gave maximum desired purity of 99%, and showed that optimal refux ratio should be decreased by

40.47%, to obtain energy efficiency gain of 28.27%, compared to the first mode.

In this study, the optimal control for the separation of a ternary mixture of 1.0-1a class, ie. one minimum boiling azeotrope mixture (ie. acetone-methanol-water) separation in two different configurations: 1) regular batch rectifier, and 2) mixed configuration composed of high-pressurized inverted column connected to the regular batch rectifier. The investigation of the influence of reboiler volume for the single column configuration was done: with the double increase of reboiler volume, there is an increase in recovery rate by 33.32% on a fixed time horizon, whereas the total recovery is achieved with time reduction by 33.34%. Moreover, there is an influence on the optimal control pattern, as the total number of cycles is increased by 34.79% too. Further, the investigation of the influence of vapor boil-up was done, to show that for an increase in vapor boil-up by 3.34 times, there is a significant reduction in total batch processing time by 20.66%. Moreover, it gives almost equal recovery rate enhancement in the overall time horizon, ie. 20.90%. Moreover, the investigation of the influence of the pressure gap on the double column configuration was done: with the decrease in top elevated pressure by 10%/20%, resp., there is a significant increase in both recovery rate, 12.09%/18.22%, resp., and in time reduction, 21.53%/31.33%, resp. Finally, both proposed schemes were verified by ChemCad dynamic simulator, and, corresponding "discontinuous heating energy curves" are defined. For the single configuration, it seems there exists a characteristic sequence after 60% of the step is completed, which can be described as "quasi zero-quasi bang- quasi bang-quasi zero-quasi bang-quasi zero-quasi bang-quasi zero". For the double column configuration, the situation is somewhat different, as the very last sequence dominates over the overall horizon as a real "bang-bang". Therefore, the overall sequence after 50% of completed step can be described as "quasi zero-quasi bang-quasi zero-quasi bang-quasi zero-quasi bang-quasi zero-bang-bang". As a final observation, the pressure gap on vacuum pressures brought a gradual improvement in the harvested distillate amount: for a decrease of vacuum pressure of only 10%, the achieved gain yielded 22.55%, even more for a decrease going from atmospheric pressure down to vacuum pressure by 50%, yielding 2.259 times.

2. PROBLEM FORMULATION

In this study, two processes with different configurations are proposed (Figure 1). In the first process, it is assumed that the distilling is made with one rectifier column, whereas the first distillation task is started with the reboiler of maximum capacity (UN) and a given volume (10 mol) of a mixture of acetone-methanol-water. The total number of stages in the first step is set at 7; however, for the second step proposed to be set at 6, and, in particular, to apply the strategy already found for the methanol-water mixture by Stojkovic et al. (2017). Hereby, the total number of stages, the same as the volume of the reboiler, is not a control variable but a predefined parameter set to its minimal value in order to reduce capital costs. The purity specified for all the main cuts is not the same, due to the existence of a minimum boiling azeotrope; therefore, in the first step, the specified purity is set at 75% (acetone recovery); however, in the second step, it is set to 95%. (methanol recovery).

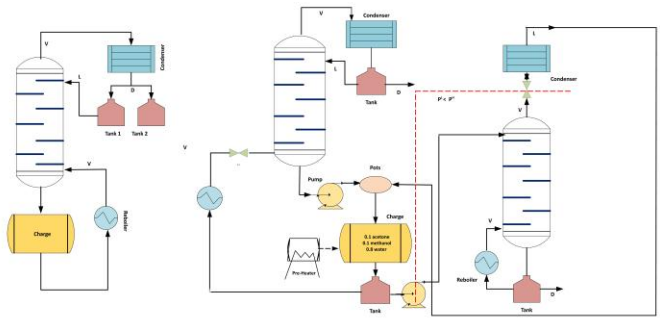

Figure 1: A scheme for ternary mixture separation with minimum boiling azeotrope: a) right – regular rectifier, b) mixed configuration: batch rectifier connected to the inverted column

Every step of the multicomponent batch distillation is finished when the most volatile component reaches its specified purity in the accumulator and/or reboiler. The campaign contains two distillations in total, i.e., the least volatile component is obtained in the reboiler after the second distillation. In contrast, the first/second, resp., component is obtained in the first/second accumulator. The operation is managed under standard atmospheric pressure to distill acetone, which is obtained in an accumulator in a desired purity of 75%, whereas the mixture containing more than 90% of methanol is obtained in a reboiler. Same as in the previous paper (Stojkovic et al. (2017)), the optimal cyclic reflux policy is implemented for binary separation. For this reason, the proposed process is suitable if the desired purified product is methanol and not acetone. In the second process, the configuration is comprised of an inverted column and a regular rectifier. The stripping step is managed under the high pressure of 10 atm to collect a mixture near azeotropic composition in the condenser to obtain purified methanol in the first tank. Furthermore, the mixture rich in acetone is left in the reboiler (>90%), whereas it is to be sent to the binary separation, where the purified acetone is obtained in a second tank. The latter process proposed is suitable if both methanol and acetone are desired purified products.

The chosen model of multicomponent batch distillation is under the following assumptions: 1) equimolar overflow, 2) total condensation, 3) vapor hold-up dynamics neglected, 4) pressure drop along the columns neglected, and 5) ideal mixing of the vapor and the liquid phase. The detailed mathematical model developed by Stojkovic et al. (2017), containing mass balances on all the parts of the batch column (MES), was extended from a binary mixture to a case of a

ternary mixture, ie. the total number of components equal to three.

The retained objective is the distillate rate defined as the total amount of the main cuts produced during the total time of the (N_{batch}=2) distillations of the operation. The optimal control problem for N_{batch} distillations is defined as:

$$\max_{R,t_f} \Sigma_{i=1}^{i=N_{batch}} \Sigma_{i=1}^{i=N_c} D_{i,j}$$

Where $D_{i,j}$ is the distillation rate for the main cut of the jth component at batch *i* and t_f is the total time for batch *i*. The optimal control problem can be described as follows: for a given multicomponent batch distillation configuration (*N* - total number of trays, *P* - working pressure), batch composition, the distillation task, and overall time horizon (t_f), determine the optimal reflux ratio to maximize the distillate at every step, subject to any constraints (model equations, bounds on the optimization variables). The problem above is a nonlinear programming problem, and, it is solved by the BOCOP solver using the direct method with a choice of discretization schemes for dynamics discretization, so to convert the problem into finite-dimensional (Cots et al. (2022)).

3. NUMERICAL RESULTS

The working conditions and predefined parameters for the first and the second process, are tabulated in Table 1, whereas concentrations are expressed from the most volatile component, acetone.

Table -1: Working conditions

Parameter	P [atm]	U_N^0 [l]	U_i^0 [l]	V [mol/h]	t_f [h]	x_N^0	$y*$
First process	1	10	0.1	11	1.6	0.1	0.75* 0.95**
Second process	10	10	0.1	11	1.6	0.1	0.65* 0.95**

*first step, ** second step

Firstly, the operation is managed under the standard atmospheric pressure (760 mm Hg), to distill acetone (75% left in the accumulator). To reach the very satisfactory recovery rate of 99.69%, a step must be repeated, which means that the total duration proposed for the best performance of the first step of the process is t_f = 2.4 [h]. The optimal control policies for the first proposed process for the separation of the minimum boiling azeotrope mixture of acetone-methanol-water in a regular rectifier are depicted in Figure 2, whereas the optimal costs and recovery rates are tabulated in Table 2, where denotes the initial mole fraction of acetone in the feed, and, denotes target mole fraction in the distillate.

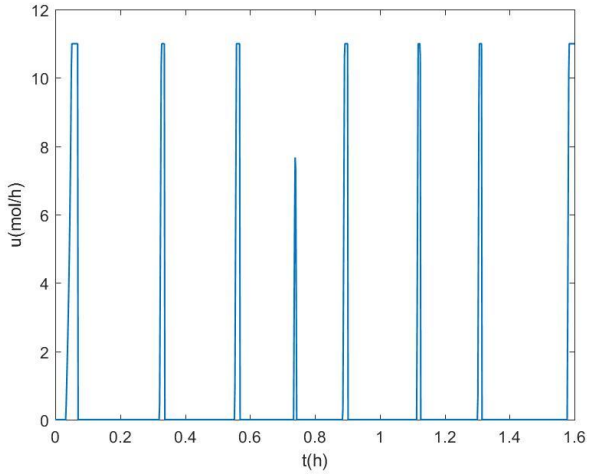

Figure 2: The optimal distillate rate $u(t)$ for the first step of the first proposed process, ternary separation

The first step, i.e., acetone distilling in a great column, begins with the shortest zero arc that lasts for even less than 0.013 [h], concatenated to a somewhat longer singular arc of 0.02 [h], followed by the initial bang arc, from the longest duration among all the other bang arcs, as it lasts 0.051 [h]. The previously mentioned pattern is never to repeat, but followed by the regular alternations between zero arcs and bang arcs: here, one can perceive that bang arcs are of almost the same duration, in contrast to the zero arcs whose duration changes with distinction. From almost the same duration are the second, the third, and the last zero arcs, i.e., their durations differ by not more than 5%. In total, the optimal control structure has four bang arcs and four zero arcs. There exist 8 commutations between different types of control.

Table 2: The optimal costs and the recovery rates

Product recovered	N	$U_0(t_f)$	Recovery rate (%)/total batch time (h)	Discr. scheme, nb. of points
Acetone (first process)	7	1.2785	1. 53.55%/0.800 2. 99.69%/ 1.493	Gauss, 2200
Methanol (second process)	8	1.2715	1.66.36%/1.600 2. 99.72%/2.400	Gauss, 2000
Acetone (second process)	8	1.7985	96.54%	Gauss, 2000

Secondly, the operation is managed under the elevated pressure of 10 [atm]. To distill methanol (65% left in the accumulator), and purified product released in the first tank. Similarly as in the previous process, a step needs to be repeated to reach the very satisfactory recovery rate of 99.72% which means that the total duration proposed for the best performance of the first step of the process is again t_f = 2.4 [h]. The total recovery rates are achieved in almost the same time, only 4.42% in favor of the simple batch rectifier configuration. The achieved recovery rate is more than 22% higher compared to those achieved by Hegely et al. (2023), who worked on extractive distillation in discontinuous mode, and close to the results obtained by You et al. (2014) and You et al. (2015), who did a separation in extractive continuous mode. The optimal control policies for the first proposed process for the separation of the minimum boiling azeotrope mixture of acetone-methanol-water in a mixed configuration are depicted in Figure 2, whereas the optimal costs and recovery rates are tabulated in Table 2.

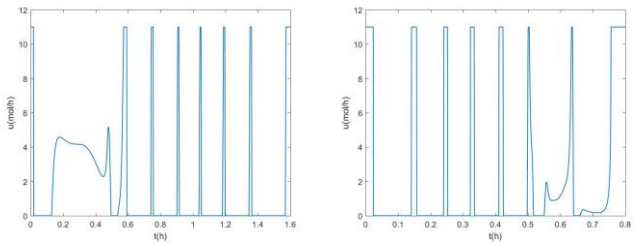

Figure 3: The optimal distillate rate for the second process: a) ternary separation, b) binary separation

In the first step, a ternary mixture of acetone-water-water is separated in an inverted column, and the optimal control structure for this part of the process is presented in Figure 3a. Again, it begins with the shortest initial bang arc, which is concatenated to the zero arc of very similar duration with all the other zero arcs except the second and last. The second zero arc is of the shortest duration among all zero arcs, whereas the last zero arc is of the longest duration, as it takes almost 12.5% of the overall time horizon. The most interesting structure actually is placed between the first and second arcs: a specific singular arc that the highest peak takes around 37.5% of the maximum achievable value and that takes the most of the time within the overall time horizon, i.e., 21.85%. In particular, this specific singular arc structure is composed of even 6 singular arcs. In total, there exist eight bang arcs, eight zero arcs, and six singular arcs. However, there are even 20 switchings between different types of the optimal control.

In the second step, a binary mixture of acetone-water is separated in a rectifier, with an acceptable recovery rate of 96.54%, and the optimal control structure for this part of the process is presented in Figure 3b. Again, the optimal control pattern begins with the bang arc, but its duration is close to the duration of the sixth bang arc and greater by at least 10% from the duration of those in the group of "equivalent bang arcs" comprised of the second, third, fourth, and fifth. The pre-last and the last sequences are the most interesting: 1) pre-last sequence is composed of three consecutive singular arcs concatenated to the bang arc, and it takes even 11.87% from the overall time horizon; 2) the last sequence is composed of a similar structure as the previous, since three consecutive singular arcs are concatenated to the bang arc, but here the complex structure of singular arcs differs with respect to the previous sequence. This is because, compared to each respective homologue in the pre-last sequence, the first singular arc peak reaches only 25% of the maximum, the second singular arc time duration is at least three times more, and the third singular arc lasts less than half as long. Moreover, the last sequence is from the longest duration, as it takes up even 17.5% of the overall time horizon. It is to note that, again as in the previous step, the first and the last zero arcs are from the exceptional duration, and all other zero arcs can be named as "equivalent zero arcs": the first/last, resp., zero arc is from the longest/shortest, resp., duration, as it takes 15%/5%, resp., of the overall time horizon.

3.1 The influence of reboiler volume

The influence of reboiler volume content on the optimal control structure will be examined for the first step of the first process, i.e., ternary separation. In Table 3 and Table 4, resp., the working conditions and the optimal costs with recovery rates for acetone, resp., are tabulated. The experiments were repeated three times, with a relative standard deviation of less than 1%. Figure 4 presents the optimal control pattern for the column functioning with double increased batch/vapor hold-up, respectively. Same as for the previous case, the pattern begins with the initial arc of the shortest duration, followed by the bang arc of the longest duration among all the bang arcs. But, in this case, the zero arcs are from almost the same duration except the fourth and the last arcs that match each other but are shorter than the rest of them for less than 20%. In both cases, we observe that the optimal control is of clear "bang-bang" type; however, the total number of zero/bang arcs increases with the simultaneous increase in both the operational parameters. This makes us believe that processing larger batches will need more commutations between different types of control within the same time frame. In summary, there exist eleven bang arcs, two "quasi-bang" arcs, and 13 zero arcs.

Table 3: Working conditions

Parameter	P [atm]	U_N^0 [l]	U_i^0 [mol]	V [mol/h]	t_f[h]	x_N^0	y*
Predefined initial value	HP: 1	20	0.1	20	1..6	0.1	0.75

Table 4: The optimal costs and recovery rates for acetone

Product recovered	N	$U_0(t_f)$	Recovery rate,[%]	Discr. Scheme, nb. of points
Acetone	7	1.9268	99.99	Gauss, 2000

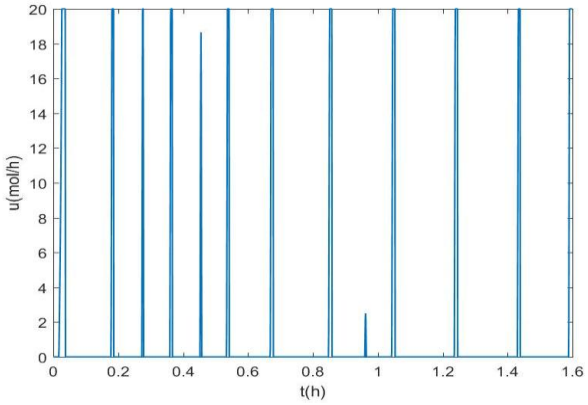

Figure 4: The optimal distillate rate for increased reboiler volume

3.2 The influence of vapor boil-up

Figure 5. presents the optimal control pattern for the column functioning with various vapor boil-ups predefined. We can observe the tendency as in the previous investigation; the increase in vapor boil-up leads to the increase of the total number of zero/bang arcs, even for the fixed batch volume. In all cases, the optimal control pattern is almost of the clear "bang-bang" type; moreover, it begins with the initial zero arc of the shortest duration, followed by a singular arc concatenated to the bang arc, and it seems that the previously described pattern is the same for all cases, but it becomes shorter with the increase of vapor hold-up. The first figure presented, going from the left to the right side, is a case for the vapor hold-up set at only 8 [mol/dm3]: one can perceive that all the zero arcs, except the first and the fourth, are from the almost same duration, as each takes somewhat less than 25% of the total batch time. Even 11 commutations between different types of control exist. After the vapor hold-up gradual increase of 1 [mol/h], the pattern becomes more complicated as the total number of bang arcs increases from five to seven in total; again, the duration of the second and seventh zero arcs is equal, as well as the third/fourth/fifth/sixth are almost from the same duration. The total number of cycles does not change much with further increase of vapor hold-up, till it reaches a value of 12 [mol/h]. Hereby, the third arc can be defined as "quasi-bang" because it reached more than 80% of the maximum. Again, for the zero arcs, one can perceive that the second, fifth, and last ones are from a close duration, whereas the third, fourth, and seventh could be seen as well as from the close duration; moreover, the latter are up to 30% shorter than the first mentioned. In this case, even 17 switchings exist. In the last case, the vapor hold-up was increased by 1 [mol/h]; consequently, the total number of cycles increased by one as well. Interestingly, third/fourth/fifth/sixth/seventh zero arcs are from the same duration, whereas the second and the last one are close in duration; the latter are up to 40% longer than the previously stated ones. The penultimate, 8th zero arc is from the greatest duration, as it takes more than 18% of the total batch time. For the last case examined, one can observe even 19 switchings between different types of control.

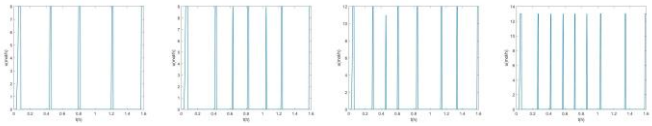

Figure 5: The optimal distillate rate **f**or the first step with the influence of vapor hold-up from left to the right side: a) V = 8 [mol/dm^3], b) V = 9 [mol/dmi^3], c) V = 12 [mol/dm^3], d) V = 13 [mol/dm^3]

In Table 5, the investigation of the vapor boil-up is presented, with different values of vapor boil-up, the achieved distillate quantities, the recovery rates, and the total number of cycles describing the optimal control pattern. Hereby the observations can be made for the ternary mixture case of minimum boiling azeotrope at atmospheric pressure, as follows: the total number of cycles changes even for a small increase in vapor boil-up [1 mol/h]; one can perceive that an increase in vapor boil-up by 2.16 times results in an increase in the total number of cycles by 55.55%. However, after some specific point, the total number of cycles does not change anymore, i.e., the optimal control structure becomes stable. On the other side, a gradual increase in vapor boil-up (1 kmol/h) is followed by the slow decrease in duration of the overall time horizon for the most acceptable recovery rate achievement (99.99%): for an increase in vapor boil-up by even 3.34 times, the time reduction is improved by 20.66%. These conclusions can lead us to project into the theoretical examination of the internal heating integration by taking into account the vapor hold-up as a second control variable.

Table 5: The investigation of the vapor boil-up

Vapor boil-up, V [mol/dm^3]	Distillate quantity, U_0 (t_f) [mol]	Recovery rate, of 99.99 %,in final time, [h]	Total number of cycles, n_c
6	1.1042	2.76	5
7	1,1496	2.67	6
8	1,1682	2.63	5
9	1,2076	2.54	7
10	1,2461	2.47	6.5

11	1,2785	2.40	7.5
12	1,3072	2.35	8
13	1,3315	2.31	9
20	1,3961	2.19	9

3.2 The influence of working pressure

3.2.1 The elevated pressure

The influence of the working pressure gap on the optimal control pattern is observed as well. In Figure 6, the cyclic strategies for the maximum working pressure set at 10 [atm] / 9 [atm], resp., are plotted in blue/red, resp. As mentioned in previous chapters, there exists a specific singular control sequence comprised of even six singular control arcs, so their durations can be compared. From Table 6, it can be perceived that with the gradual decrease of the pressure gap, this specific singular control sequence tends to last longer: if the pressure gap decreases by a single unit, then its duration increases by 22.23%, however, for further decreases, it tends to show even more. The interesting fact is that, with the gradual decrease in working pressure gap (1 [mol/h]), the recovery rate increases on a regular basis, i.e., it shows to increase by 18.22%/12.09%, resp.

Table 6: The investigation of the elevated pressure

Total pressure, [atm]	Distillate quantity, [mol], $U_0(t_f)$	Recovery rate, of 99.99 %,in final time, [h]	Total number of cycles, n_C	Complex sequence duration, [h]
8	1,8496	0,8274	4	0.95
9	1,6206	0,9457	8	0.45
10	1,2715	1,2054	8	0.35

In order to validate the results, ChemCad 6.1, a dynamic simulator, is employed to design the identical cyclic optimal reflux strategy obtained by Bocop for both processes over the predefined time horizon. Afterward, from the dynamic simulation, the "discontinuous heating energy function" is extracted. In Figure 7, the optimal reboiler duty vs. time, the extracted values are presented for the step for the ternary separation that occurred for the first and second processes, respectively. The thermodynamic model used in ChemCad is NRTL, and the mass balance tolerance is ±0.001 [kmol/h].

In Figure 7a, the discontinuous heating function for the first step in ternary separation under standard atmospheric pressure is presented. Although the minimum total energy requirement is obtained as 73,650 (kJ/mol). Hereby, it is to follow the heating strategy as described: after the initial reboiler duty is imposed, in the second step, it needs to be decreased by at least 1.8 times; afterwards, it needs to be increased by at least 2.5 times. After this particular moment, a stepwise gradual increase would be imposed of not more than 1.5% until the process reaches its midpoint. From here, a "quasi bang-bang" politics should be applied: consecutive steps switching from an increase/decrease, resp., by 5.5/5.7 times, resp., and 5.9/6.1 times, resp. In the pre-last step, the long-term extreme decrease by 72 times should be simulated.

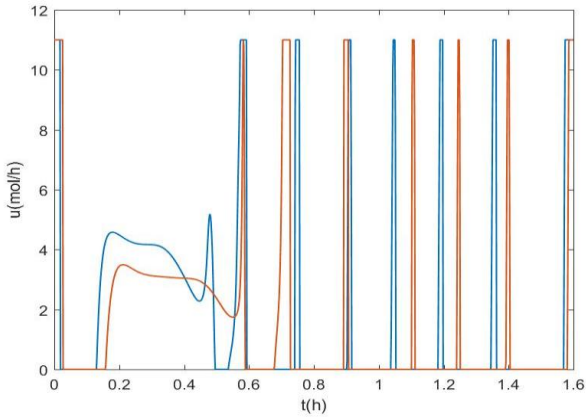

Figure 6: The working pressure influence: blue line – elevated wokring pressure set at 10 [atm], red line – elevated working pressure set at 9 [atm]

In Figure 7b, the discontinuous heating function for the first step in ternary separation at elevated pressure is presented. For the presented reboiler duty function, the proposed heating strategy was as follows: after the initial reboiler duty was imposed, in the second step, it needed to be decreased by at least six times; afterward, it needed to be increased again by almost eight times. After this particular moment, a stepwise gradual increase was imposed of not more than 1.5% until the process reached its midpoint. From this particular moment, a "quasi bang-bang" politics should be applied: the value should be increased by four and six times in two consecutive steps, then again decreased by six times. Afterwards, an even greater step should be applied, as an increase of 6.1 times in the next step is followed by a decrease of 6.3 times and, consecutively, an increase of 6.5 times. Hereby, the pre-last step should be simulated by a long-term decrease of even 77 times, and the final step should be a stable maximum achieved value found after increasing the value by 166.1 times. From here, the minimum total energy requirement is obtained as 75,750 (kJ/mol).

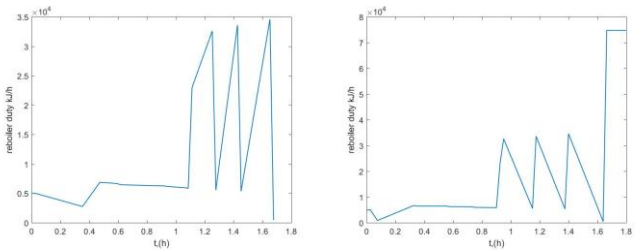

Figure 7: The optimal reboiler duty vs time for: a) under atmosperic working pressure in rectifier, b) at elevated working pressure in inverted column.

3.2.1 The vacuum pressure

The first part of the pressure-swing distillation process presented in the previous chapters, operated at a total pressure of atmospheric pressure, can also be operated under vacuum. Notably, the investigations were expanded to the values set at 0.5 [atm] / 0.6 [atm]. The temperatures on the stages are plotted: one can observe that the range of temperature goes between 37.0462°C and 45.4800°C for the process under the vacuum set at 0.5 [atm] (Figure 8a) and between 41.6152°C and 49.2229°C for the setup at 0.6 [atm] (Figure 8b), which complies with the findings of You et al. (2015).

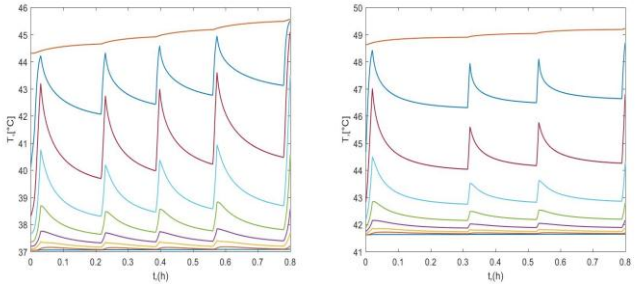

Figure 8: Temperatures on the trays for vacuum rpocesses: a) pressure set at 0.5 [atm], b) preesure set at 0.6 [atm]

To assess the influence of vapor boil-up on the optimal control structure and recovery rate, this parameter is varied (see Table 7). The optimal control patterns for vapor boil-up varied are displayed on Figure 9/Figure 10, resp., for vacuum total set up at 0.5 [atm]/0.6 [atm], resp. The main solution obtained for the lowest value of vapor boil-up (Fig. 9a), for the pressure set at 0.5 [atm], has an initial double singular arc of very short duration, followed by a clear bang-bang policy, having 10 commutations between different types of control, whereas the last arc corresponds to a maximum distillate. The situation is similar for the other cases, where the total number of internal arcs is to increase by a rule. If remember the previous chapter, even a small change in vapor boil-up had a significant influence on both the optimal control structure and recovery rate, but, in the case of vacuum pressures, only after significant increase in vapor boil-up the changes in control pattern are visible where the recovery rate remains almost constant. Still, the total time for a maximum recovery rate shows to be reduced by even 22.55% compared to the case of vacuum pressure set at 0.6 [atm], and even 2.259 times reduced compared to the process managed under atmospheric pressure (1 [atm]). With a further increase in total pressure, these achievements do not change significantly.

Table 7: The investigation of the vacuum pressure

Total pressure, [atm]	Vapor boil-up, V [mol/h]	Distillate quantity, [mol], $U_0(t_f)$	Recovery rate, of 99.99 %,in final time, [h]	Total number of cycles
0.5	11	0.9705	1.0622	5
	15	1.0813	1.0328	6
	19	1.1593	1.0709	8
0.6	11	0.5938	1.3716	4
	15	0.6172	1.3618	5
	19	0.6335	1.3516	6

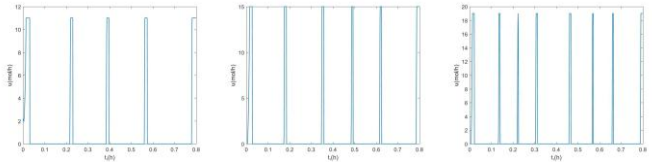

Figure 9: The optimal control for vapor boil-up set up at 0.5 [atm]: a) V = 11 [mol/dm^3], b) V = 15 [mol/dm^3], c) 19 [mol/dm^3].

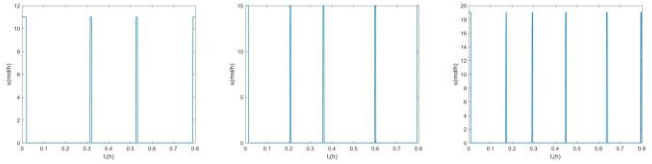

Figure 10: The optimal control for vapor boil-up set up at 0.6 [atm]: a) V = 11 [mol/dm^3], b) V = 15 [mol/dm^3], c) 19 [mol/dm^3].

The optimal control structure for the pressure set at 0.6 [atm] for the lowest value of vapor boil-up (Fig. 10a) is shown to begin and terminate with a bang arc, with only two internal bang-zero sequences. There are 6 commutation between different types of control. The same structure appear with an increase in vapor boil-up (Fig. 10b), where the total number of internal arcs is to increase more slowly than in the previous case. Finally, the optimal control pattern changes in its final sequence (Fig. 10c) appear to be zero arc, so there are 11 commutations between different types of control. The interesting fact is that, with the gradual decrease in working pressure gap (4 [mol/h]), the recovery rate increases on a regular basis, but only for less than 2%. As we could see, in all cases, vapor overhead as a main driving force has a significant influence on the separation task: if total pressures are set at atmospheric and/or lower than atmospheric pressure, there is a visible impact on the optimal control structure with some additional improvements in gain, as a double effect. Moreover, at the vacuum pressures of 0.5 [atm] / 0.6 [atm], resp., the azotrope acetone mole fraction moves to 87%/85%, resp.,

which makes it possible to obtain the azeotropic mixture in the accumulator with increased content of lower boiler. With a clear difference from the first process described in the previous chapters, managed under atmospheric pressure, the vacuum processes can be recommended as a possible solution for distilling both high-purity products.

4. CONCLUSIONS

The optimal control strategy for the separation of a 1.0-1a class mixture, a minimum boiling azeotrope of acetone-methanol-water in different configurations, namely, a regular batch rectifier and a mixed configuration comprised of a high-pressurized inverted column connected to the regular batch rectifier, is the subject of this work. When it comes to the recovery rate, both schemes show the most acceptable outcome for both products. However, in terms of final product purification efficiency, the double column scheme outperformed the single column one, since both highly purified products were possible to distill. The investigation of the influence of reboiler volume and vapor boil-up was done for the single column configuration, and the investigation of the influence of pressure gap for the double column configuration. The influence of reboiler volume brings real close improvement in both recovery rate and time reduction, by 33.32%, whereas the total number of cycles is increased by 34.79%. Hence, the influence of vapor boil-up showed that with the increase of vapor boil-up by 3.34 times, there is a significant increase in both recovery rate and time reduction, resp., by 20.90%/20.66%, resp. Also, for an increase in vapor boil-up by 2.16 times, the total number of cycles increases by 55.55%. The influence of the pressure gap on elevated pressures on the double column configuration: the decrease in elevated top pressure by only 10%/20%,resp., brings significant improvements in both recovery rate, 12.09%/18.22%, resp., and time reduction, 21.53%/31.33%, resp. Moreover, the specific complex singular control sequence is detected, comprising six singular arcs, with a tendency to last longer with pressure decrease. Following the validation procedure, the "discontinuous heating function" was derived, giving a clear idea that the process could be controlled by reboiler duty: repetitive "quasi-bang-quasi-zero" sequences are perceived, as well as a real bang-bang sequence. Lastly, the pressure gap influence on vacuum pressures: the decrease in vacuum pressure for only 10% brings at least 22.55% in gain for a yield; even more important are gains when going down from atmospheric pressure, where the decrease by 50% brought an increase in yield by even 2.259 times.

REFERENCES

1) You, X., Rodriguez-Donis, I., & Gerbaud, V. (2014). Extractive distillation process optimization of the 1.0-1a class system, acetone-methanol with water. Comp. Aid. Chem. Engng. 33, 1315-1320. doi.org/10.1016/B978-0-444-63455-9.50054-4

2) You, X., Rodriguez-Donis, I., & Gerbaud, V. (2015). Improved design and efficiency of the extractive distillation process for acetone–methanol with water. Ind. Eng. Chem. Res., 54(1), 491-501. doi.org/10.1021/ie503973a

3) Daosud, W., Jariyaboon, K., Kittisupakorn, P., & Hussain, M.A. (2016). Neural network based model predictive control of batch extractive distillation process for improving purity of acetone. Engineering Journal, 20(1), 47-59. doi.org/10.4186/ej.2016.20.1.47

4) Tututi-Avila, S., Medina-Herrera, N., Hahn, J., & Jiménez-Gutiérrez, A. (2017). Design of an energy-efficient side-stream extractive distillation system. Comp. Aid. Chem. Engng., 102, 17-25.. doi.org/10.1016/j.compchemeng.2016.12.001

5) Mangili, P. V., Souza, Y. P., de Menezes, D. Q., Santos, L. S., & Prata, D. M. (2018). Eco-efficiency evaluation of acetone-methanol separation processes using computational simulation. Chemical Engineering and Processing-Process Intensification, 123, 100-110. doi.org/10.1016/j.cep.2017.10.022

6) Frolkova, A., Frolkova, A., & Gaganov, I. (2021). Extractive and Auto-Extractive Distillation of Azeotropic Mixtures. Chemical Engineering & Technology, 44(8), 1397-1402. doi.org/10.1002/ceat.202100024

7) Zhao, F., Xu, Z., Zhao, J., Wang, J., Hu, M., Li, X., & Ma, Y. (2021). Process design and multi-objective optimization for separation of ternary mixtures with double azeotrope via integrated quasi-continuous pressure-swing batch distillation. Separation and Purification Technology, 276, 119288.

8) Schöneberger, J. C., Staak, D., & Rarey, J. (2022). Solvent recovery by batch distillation - Application of multivariate sensitivity studies to high dimensional multiobjective optimization problems. Simulation and Optimization in Process Engineering, 101-142. doi.org/10.1016/B978-0-323-85043-8.00003-9

9) Zhang, F., Sun, D., Li, Y., Shan, B., Ma, Y., Wang, Y., & Zhu, Z. (2022). Heat integration and dynamic control for separating the ternary azeotrope of butanone/isopropanol/n-heptane via pressure-swing distillation. Chemical Engineering and Processing-Process Intensification, 170, 108657. doi.org/10.1016/j.cep.2021.208657

10) Miao, G., Zhuo, K., Li, G., & Xiao, J. (2022). An advanced optimization strategy for enhancing the performance of a hybrid pressure-swing distillation process in effective binary-azeotrope separation. Separation and Purification Technology, 282, 120130. doi.org/10.1016/j.seppur.2021.120130

11) Seihoub, F.Z., Gerbaud, V., & Benyounes, H. (2024). Automated method for designing extractive dividing column used to separate minimum azeotropic mixtures with a heavy entrainer. Chem. Eng. Res. Des., 207, 361-372. doi.org/10.1016/j.cherd.2024.05.041

12) Ai, S., Qin, Y., Liu, L., & Yu, W. (2023). Reaction-assisted separation of acetone from the azeotrope of methanol and acetone. Chemi. Eng. Res. Des., 193, 507-515. doi.org/10.1016/j.cherd.2023.04.010

13) Hegely, L., Karaman, Ö. F., Szucs, M. T., & Lang, P. (2023). Surrogate model-based optimisation of a batch

distillation process. Chem. Eng. Res. Des., 192, 456-467. doi.org/10.1016/j.cherd.2023.02.043

14) Hegely, L., & Lang, P. (2023). Optimisation of the higher pressure of pressure-swing distillation of a maximum azeotropic mixture. Energy, 271, 126939. doi.org/10.1016/j.energy.2023.126939

15) Hegely, L., Nemeth, B. & Lang, P. (2025). Isopropanol dehydration by batch extractive distillation under variable pressure. Separation and Purification Technology, 369, 133178. doi.org/10.1016/j.seppur.2025.133178

16) Hegely, L.; Lang, P. (2025). Surrogate Model-Based Optimization of Pressure-Swing Distillation Sequences with Variable Feed Composition. Systems and Control Transactions, 192-197. doi.org/10.699997/sct.161606

17) Karaman, Ö. F., Lang, P., & Hegely, L. (2025). Optimisation of pressure-swing distillation of a maximum-azeotropic mixture with heat integration. Energy, 320, 135190. doi.org/10.1016/j.energy.2025.135190

18) Luyben, W. L. (2025). Drastic Impact of Pressure on Energy Consumption in a Xylene-Splitter Distillation Column. Ind. Eng. Chem. Res., 64(38), 18976-18978. doi.org/10.1021/acs.iecr.5c02518

19) Liang, S., & Bu, G. (2024). Comparison of different heat integration pressure swing distillation processes for separating isobutanol and p-xylene azeotrope. Scientific Reports, 14(1), 28472. doi.org/10.1038/s41598-024-79870-6

20) Wen, G., Li, F., Wu, H., Tang, G., Lu, W., Wang, Y., & Li, X. (2025). Separation performance and controllability improvement for pressure-swing distillation based on the relationship between feed composition and distillation boundaries. ACS Sustainable Chemistry & Engineering, 13(20), 7493-7508. doi.org/10.1021/acssuschemeng.5c01048

21) Mahida, B., Benyounes, H., Medjahdi, M., Mokhtari, M., & Khelifa, I. (2025). Optimization and feasibility analysis of pressure swing distillation for the separation of formic acid, propionic acid, and water azeotropic mixture. Journal of King Saud University–Engineering Sciences, 37(4), 12. doi.org/10.1021/bp980026i

22) Jassim, M., Aqar, D. Y., & Ahmed, S. M.(2025). Simulation Study of Methyl Salicylate Production via Reactive Distillation Columns. Journal of Petroleum Research and Studies, 15(2), 106-125. doi.org/10.52716/jprs.v11i2.496

23) Stojkovic, M., Gerbaud, V., & Shcherbakova, N. (2017). Batch distillation of binary mixtures: preliminary analysis of optimal control. IFAC-PapersOnLine, 50(1), 4899-4904. doi.org/10.1016/j.ifacol.2017.08.743

24) Cots, J.B.C.O., Martinon, P., Caillau, J.B. & Cots, O. (2022). ct: control toolbox–Numerical tools and examples in optimal control.